DEVELOPMENT OF A TEST DEVICE FOR THE EVALUATION OF HYDRODYNAMIC LUBRICATION IN THRUST BEARINGS

AAPO PASANEN, JAAKKO KLEEMOLA* AND ARTO LEHTOVAARA
Tampere University of Technology, Mechanics and Design
P.O. Box 589, 33101 Tampere, Finland
* corresponding author: jaakko.kleemola@tut.fi

ABSTRACT

Oil lubricated thrust and journal bearings are widely used in industrial machines such as in stone crusher applications. In this study, a laboratory-scale test device for the evaluation of hydrodynamic lubrication in thrust bearings is developed. In the test device, the normal load, rotation speed, lubricant supply temperature and inlet flow rate can be adjusted and measured continuously and independently. In addition, thrust plate temperature and friction torque can be measured. This allowed initial testing of the functionality of the transient hydrodynamic model, which had been developed earlier to enhance bearing design and the testing process. The results show that the trends of the measured and the calculated results correspond well. The absolute friction coefficient values are also in reasonable agreement. The obvious main cause for deviation of results is the oil temperature in the pad inlet, exact estimation of which, by theoretical or experimental means, is complicated.

Keywords: hydrodynamic lubrication, thrust bearing, test device

INTRODUCTION

Oil lubricated thrust and journal bearings are widely used in industrial machines such as in stone crusher applications. The crushing process causes high dynamic peak loads to bearings, which complicates the bearing design. Bearings can be oversized, but this causes unnecessary friction and power loss as well as the need for additional oil flow, which lowers the total efficiency of the crusher. In crusher applications, bearing optimization is in general very challenging and expensive measurements, with long lasting full-scale tests, are required to validate the design.

To enhance the bearing design and testing process, advanced design tools have been developed /Lehtovaara, 2005, 2006, 2007/. These are the three-dimensional transient models for the numerical evaluation of the hydrodynamic lubrication of thrust and journal bearings with reasonable calculation times. The numerical methods are preferred because bearing side leakage, dynamic operation conditions, thermal effects and shaft misalignments must be considered. An analytical solution for hydrodynamic lubrication of these bearings can only be found for very limited operating conditions and bearing geometry. The theoretical aspects and main properties of hydrodynamic bearings can be found for example in references /Hamrock, 1994/ and /Stachowiak and Batchelor, 1993/ and /Esdu, 1982/.

Experiments were needed to obtain measured data for bearing behaviour and to test the model for design purposes. As a first step, laboratory-scale experiments were preferred. In this study, a laboratory-scale test device for the evaluation of hydrodynamic lubrication in thrust bearings is developed. Further, the functionality of the model and the test rig as well as the input values for the model are evaluated by comparing experimental and model results.

EXPERIMENTAL

Test device

The test rig is built on a thick steel plate and it consists of an electric motor, a shaft, test bearing, thrust plate, connector, hydraulic load cylinder and lubrication unit as shown in Fig. 1.

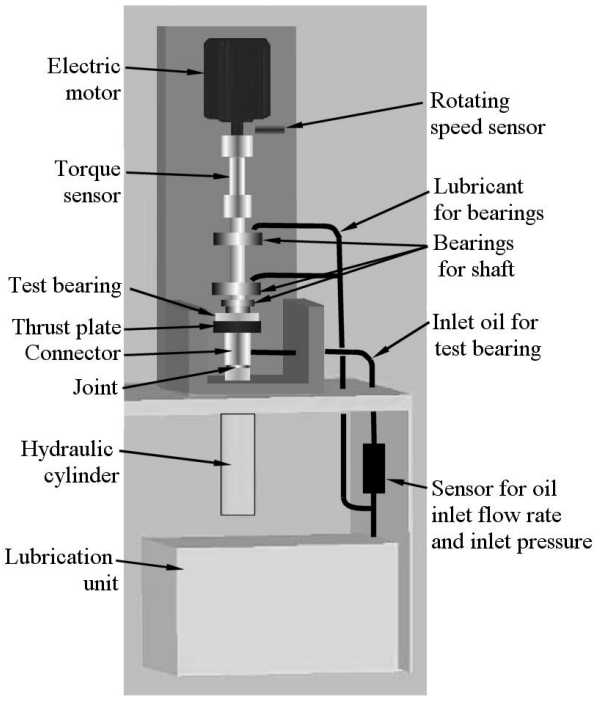

Figure 1. Principle of the test rig.

An electric motor rotates the shaft, which is supported by two ball bearings for radial forces and by one ball bearing for axial forces. The test bearing is attached to the end of rotating shaft. The loading of the test bearing is generated by the hydraulic cylinder, which is attached via a connector to the thrust plate. Lubricant is supplied to the test bearing through the connector and a hole in the middle of the thrust plate as shown in Fig. 2. The connector is attached via a joint on the top of the hydraulic load cylinder ensuring parallel contact between the test bearing and the thrust plate.

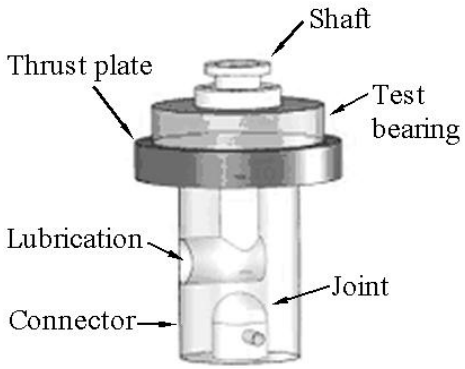

Figure 2. Bearing installation.

The lubrication unit circulates lubricant through the test bearing and controls the oil inlet flow rate, pressure and supply temperature. A separate lubrication line is arranged for the shaft bearings.

Test bearing

A fixed-pad type thrust bearing consists of a steel thrust plate and a sector-shaped bearing with fixed load carrying pads, as shown in Figure 3.

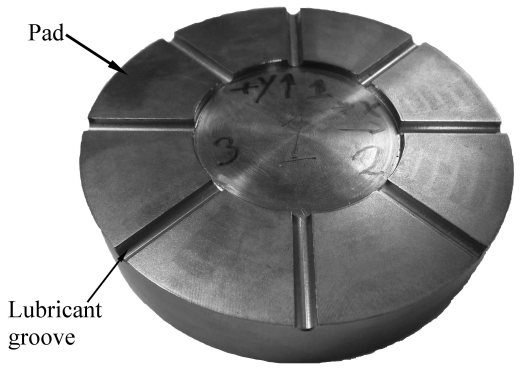

Figure 3. Test bearing geometry.

The bearing was made of bronze and is divided into eight pads. The bearing outer and mean diameters are 100 mm and 75 mm, respectively. Lubricant is supplied to the middle of the bearing as described earlier. Lubricant that does not enter the contact area flows out through the grooves. Under steady-state conditions, hydrodynamic lubrication takes place between the rotating pads and the thrust plate as lubricant enters the converging wedge-shaped pad geometry, i.e., a physical wedge pressure-generating mechanism operates. In a transient situation, a squeeze film effect may temporally maintain the lubrication film. The detailed geometry of the pad and the plate is shown in Fig. 4.

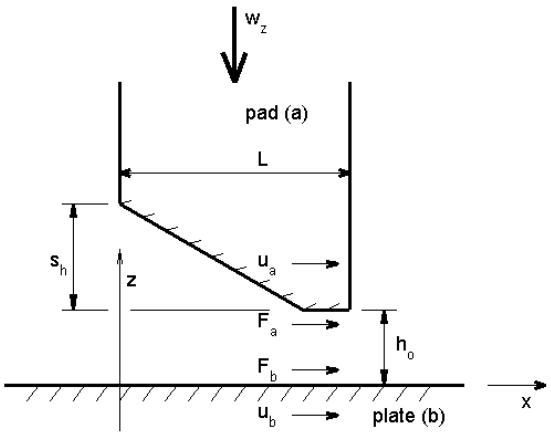

Figure 4. Geometry between pad and plate.

The length of the each pad L is 25 mm at the mean diameter, where the inclined part is 20 mm and the land part at the pad outlet is 5 mm. The width of the pad b is 20 mm. The shoulder height s_h i.e., taper rise of the inclined part pad had a design value of 50 μm. Because the shoulder height is a crucial parameter in bearing design, the geometry of the three pads was measured using a coordinate measurement device. The measured pad shoulder geometry was observed to be well within the required tolerance. In numerical calculations, a pad shoulder value of 47 μm will be used, based on the measured results. The pad was modeled as a rectangular area, where the one side of the rectangle is the length at the mid point of the sector shaped pad (L) and the other side of rectangle is b. The use of rectangular pad data for the design and analysis of bearings with sector shaped pads does not lead to errors of practical significance with sector angles of up to 45° /Esdu, 1982/.

The configuration of a bearing rotating against a fixed plate was chosen to allow the option in the future of installing additional sensors on the thrust plate to monitor the distribution of oil film thickness and pressure if necessary. The rotating bearing will cause some additional churning losses if only at high operating speeds.

The test rig was calibrated by replacing the test bearing with the axial force ball bearing similar to the existing one that takes the shaft axial forces. The effect of a possible small radial runout from the axial bearing to the radial ball bearings was eliminated by positioning eight loose bearing balls below the axial bearing. This floating attachment approximately acts in a similar way to the lubricated test bearing. The test rig was operated with this setting in all test case conditions, which included losses from two axial and two radial bearings. The share of the

power loss arising from shaft radial bearings was determined and eliminated by rotating the device in the test cases without a load. In this way, the power loss of the shaft related axial and two radial force bearings can be measured in every test case and excluded from the results. The external bearing losses were between 6-24 % of the total losses, so that the calibration procedure was considered to be reasonably accurate.

Measured signals

The normal load was measured by pressure sensor for the hydraulic cylinder. This loading system was calibrated with a separate force sensor before the actual measurements. The oil supply temperature was measured with a thermo element 50 mm before the test bearing contact. The controller maintained the temperature fluctuations within ± 1 ºC. The thermo elements with amplifiers were calibrated with a laboratory thermometer in every 10 degrees in a temperature range of 30-90ºC. The bearing sliding velocity can be adjusted by varying the speed of the electric motor which was controlled by a frequency transformer. The motor speed was measured continuously with a tachometer on the shaft, having been initially checked with another tachometer straight on the head of the motor shaft. Oil flow rate was measured by oil flow sensor, which has known calibration values. The thrust plate temperature was measured with a thermo element placed 1mm below the thrust plate sliding surface. The thermo element was located on the central line of the bearing pads. Friction torque was measured with a stain gauge-based sensor located next to the electric motor. The torque sensor was calibrated using a torsion arm and weights after each set of measurements at a given temperature had been completed.

Lubricant

Gear lubricant of class ISO VG 150 was used. This mineral oil was filteted by using a 3µm filter. Lubricant viscosity was measured with capillary viscosity meter at every measurement temperature and average values from three separate measurements are shown in Table 1.

Table 1. The test lubricant viscosity (mm^2/s).

	40 ºC	50 ºC	60 ºC
1	149.5	86.3	58.7
2	147.8	89.4	56.3
3	148.0	84.4	56.6
Average	148.4	86.7	57.2

The results are within the range given by the oil manufacturer. The lubricant specific heat c_p and density ρ is assumed to be constant, so that $c_p*\rho$ = 1.7E6 J/(m^3 K). The effect of pressure on viscosity is ignored.

Test matrix

The test matrix was designed to fulfil the demands of the Taguchi method /Taguchi, 1987/. The nine experimental test cases each with four main parameters (load, sliding velocity, oil inlet flow rate and supply temperature) form a L_9 orthogonal array as shown in Table 2. After each set of tests the test was repeated with calibration settings in order to eliminate the effect of external bearing losses. Pure hydrodynamic lubrication conditions were sought in the tests.

Table 2. The test matrix.

Case	Mean pressure (MPa)	Velocity (m/s)	Oil inlet flow rate (l/min)	Oil supply temperature (°C)
1	0.5	3	1	60
2	0.5	5	2	50
3	0.5	8	3	40
4	1	3	3	50
5	1	5	1	40
6	1	8	2	60
7	2	3	2	40
8	2	5	3	60
9	2	8	1	50

Before the measurements begun, oil was circulated over the night at the test temperature. A set of tests at one temperature were measured in sequence. Before each test temperatures were stabilized. The measurement time for each test was 20 min. All measured data was stored and later analysed. Sampling frequency was 2 Hz for temperature and velocity measurements.

RESULTS AND DISCUSSION

The actual friction torque in the test bearing was obtained by subtracting the measured external bearing torque from the measured total friction torque. The friction force was calculated by dividing the test bearing friction torque by the torque arm, which was calculated from the centre of the pads' surface area. The friction coefficient was obtained by dividing friction force to normal force and the power loss by multiplying friction force with sliding speed at the centre of the pads. The test bearing friction coefficient, temperature, friction torque and power loss are shown in Table 3.

Table 3. Results of the measurements.

Case	Friction coefficient	Thrust plate temperature (°C)	Friction torque (Nm)	Power loss (W)
1	0.010	68	0,955	73
2	0.0102	63	0,972	124
3	0.0190	55	1,82	374
4	0.0071	59	1,35	104
5	0.0073	71	1,40	179
6	0.0082	74	1,57	322
7	0.0052	66	2,00	154
8	0.0050	72	1,93	248
9	0.0049	89	1,90	389

In test case 1, the bearing did not work optimally because of the extreme combination of operating values. In case 3, the friction coefficient is very high due to the high sliding velocity combined with low oil supply temperature.

The comparison of the model and the experimental results

A three-dimensional transient model for hydrodynamic lubrication of fixed thrust bearings has been developed earlier /Lehtovaara, 2005/. Only a brief outline is presented here. The solution is based on the Reynolds equation by assuming Newtonian fluid and incompressible lubricant as follows:

$$\frac{\partial}{\partial x}\left(h^3\frac{\partial p}{\partial x}\right)+\frac{\partial}{\partial y}\left(h^3\frac{\partial p}{\partial y}\right)=6\eta_e u_b\frac{\partial h}{\partial x}+12\frac{\partial h}{\partial t} \quad (1)$$

In addition to the film thickness h and the pressure distribution p, the model calculates friction, fluid flow rate, power loss and temperature, which are based on an effective temperature approach. The plate shear force F_b for one pad in the x-direction is expressed as:

$$F_b = \int_{-b/2}^{b/2}\int_{0}^{L}\left(-\frac{h}{2}\frac{dp}{dx}-\frac{\eta_e u_b}{h}\right)dxdy \qquad (2)$$

The friction coefficient f is the friction force F_b divided by the normal force and the power loss h_p is the friction force F_b multiplied by sliding velocity. Assuming that all the heat produced by the viscous shear is carried away by the lubricant, the bulk temperature rise of the lubricant ΔT is given as:

$$\Delta T = \frac{h_p}{\rho q c_p} \qquad (3)$$

The effective temperature T_e within the lubricant is approximated to be:

$$T_e = T_{in} + \Delta T/2 \qquad (4)$$

The effective viscosity η_e of mineral oil is described as a function of the effective temperature T_e for an ISO VG-class lubricant.

The numerical model developed had already been tested successfully against literature examples, which means that the program code obeys the laws presented by the theory. The next step was to compare the model results with the experimental results. This will demonstrate the functionality of the model and the test rig as well as the input values given to the model.

Most of the model input values can be determined fairly easily and exactly. However, the numerical model needs the oil temperature at the pad inlet as an input value. It is known to be a very difficult task to estimate this theoretically. A varying amount of the hot oil carry over will take place, where a portion of the hot lubricant discharged from one pad is entrained in the following pad mixing with the "cold" lubricant supplied. The models for hot oil carryover do not take account of oil flow rate to the bearing /Almqvist et. al., 2000/. To overcome these difficulties, the thickness of the hot oil carryover layer was deduced experimentally resulting in a fraction of 44 % of the entering oil film thickness in the studied application /Almqvist et. al., 2000/. However, this ratio is dependent on the application and on the operating conditions.

In this study, the tests do not have classical oil path or direct lubrication conditions since the oil was fed into the centre of the bearing and it reaches the pads trough the bearing grooves as the bearing rotates. The excess oil flows out from the bearing through the bearing grooves. The test arrangement has a thermo element near the thrust plate sliding surface to get some indication of temperature behaviour trends under different operating conditions. This was also utilized when estimating the oil inlet temperature to the pads with the model calculations as follows:

$$T_{in} = (T_{su} + T_p)/2 \qquad (5)$$

where T_{su} is the measured oil supply temperature to the bearing, and T_p is the measured thrust plate temperature. It is obvious that this equation is an approximation. Even so, it would be a useful feature for designers, if the model and experiments show similar kinds of behaviour trends.

The model was used to calculate figures for the nine cases and the results are shown in Figures 5 and 6 together with the experimental results. A large range of operating conditions was tested in the experiments. As stated earlier, the test Case 1

suffered slightly from extreme operating conditions, which is seen in the higher friction coefficient in Fig. 5.

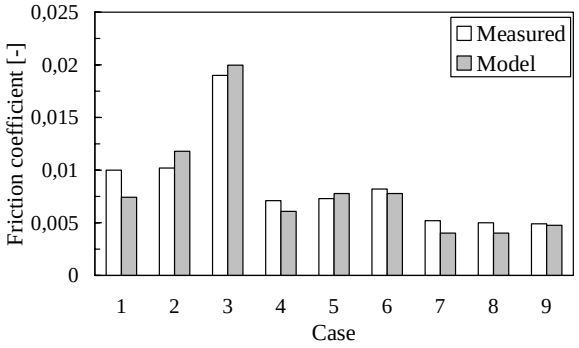

Figure 5. The thrust bearing friction coefficient at different operating conditions.

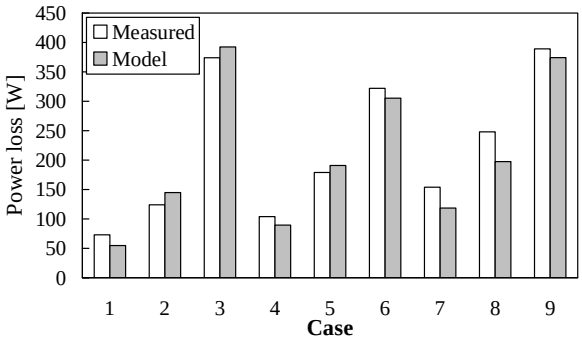

Figure 6. The thrust bearing power loss at different operation conditions.

Figs 5 and 6 show that the behaviour trends of the measured and the calculated results correspond well. Even the absolute values of friction coefficients are in reasonable agreement. The mean relative difference in friction coefficient is 11 % in cases 2-9. The maximum difference occurs in case 7, where it is 23 % from the measured value. The main source of deviation of the results is obviously the oil temperature at the pad inlet. Another source for deviation may be churning loss, which exists in experiments, but in slow or moderate sliding speeds it plays a minor role. A possible source of error in the model is its use of an effective mean temperature.

Trend analysis

The first requirement for a reliable design tool is that it is able to give correct trends for the main parameters involved in the system. The Taguchi method /Taguchi, 1987/ was applied in experiments to obtain the general trends for the effects of the main parameters (load, velocity, oil supply temperature, oil flow rate) on the mean response of hydrodynamic friction, power loss and temperature difference. Each of the four main parameters consists of three levels. The target in using the Taguchi method was to gain appropriate data on the trends with a minimum number of experiments. The corresponding results were also simulated with the numerical model. The results for load (mean pressure) induced trends are shown in Figures 7 and 8. In load induced calculations, mean values of sliding velocity and oil supply temperature was used.

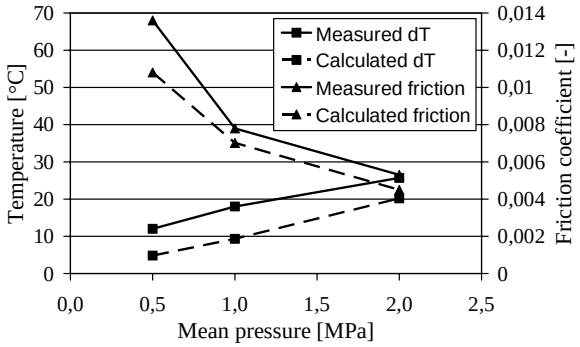

Figure 7. Friction coefficient and temperature difference trends as a function of mean pressure.

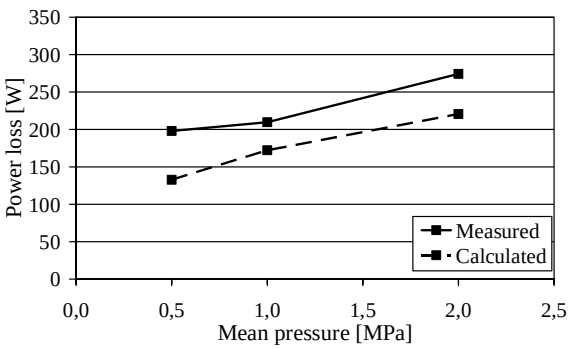

Figure 8. Power loss trends as a function of mean pressure.

The results in Figure 7 and 8 show that similar trends for response parameters are obtained from the experimental and the numerical results. The temperature difference *dT* based on measurements represents the balance of thrust plate and lubricant supply temperatures. In the calculations, it represents the temperature rise in the contact i.e. Eq. 3. In the measured trend, the slight deviation upwards at 0.5 MPa load is obviously due to the high friction result in the Case 1. Good correlations were also obtained with other main parameters induced trends, excluding the differences caused by the Case 1 result.

Trend analysis revealed that increased oil inlet flow rate and decreased oil supply temperature reduce the thrust plate temperature. This increases friction and power loss, but it also decreases the risk of bearing failure. The oil flow rate is not a direct input value in the model. This was taken into account through control of the oil supply temperature. More comprehensive temperature analysis requires use of energy and heat transfer equations resulting in solutions that are more structure and application dependent. However, experiments are still needed to deduce the heat transfer and conduction coefficients as well as the amount of hot oil carry over for the model input values.

CONCLUSIONS

The test device was developed for the evaluation of the hydrodynamic thrust bearings. The normal load, rotation speed, lubricant supply temperature and inlet flow rate can be adjusted and measured continuously and independently. In addition, the thrust plate temperature and friction torque are measured.

The analysis by the Taguchi method shows that the behaviour trends of the measured and the calculated results correspond well. The absolute friction coefficient values are also in reasonable agreement. In eight measured cases, the mean relative difference in friction coefficient is 11 % and the maximum difference is 23 % from the measured value. The main source for deviation in the results is obviously the oil temperature at the pad inlet. This is the model input value for which exact estimation, either by theoretical or experimental means, is the most complicated.

ACKNOWLEDGEMENTS

The authors are grateful for permission to publish this paper and for the financial support provided by Metso Minerals Oy.

NOMENCLATURE

b = pad width in y-direction
c_p = specific heat of lubricant
f = friction coefficient
F_a = shear (friction) force in x-direction, surface a
F_b = shear (friction) force in x-direction, surface b

h = lubricant film thickness
h_o = outlet film thickness
h_p = pad power loss

L = pad length in x-direction
p = fluid film pressure
p_{me} = mean pressure ($w_z/(L*b)$)
q = volumetric flow rate

s_h = pad shoulder height
t = time
T_e = effective temperature
T_{in} = pad inlet temperature
T_{su} = lubricant supply temperature
dT = temperature difference
ΔT = lubricant temperature rise

u_a = surface a (pad) sliding velocity in x -direction
u_b = surface b (plate) sliding velocity in x -direction
VG = lubricant ISO VG-class
w_z = pad normal load

x = coordinate in the direction of sliding motion
y = coordinate, transverse to the direction of sliding motion
z = coordinate across the fluid film
η_e = effective absolute viscosity
ρ = lubricant density

REFERENCES

[1] Almqvist, T., Glavatskikh, S. B., Larsson, R., THD Analysis of Tilting Pad Thrust Bearings – Comparison Between Theory and Experiments, ASME J. Trib. 122 (2000) 412-417.

[2] ESDU 82029, Calculation Methods for Steadily Loaded Fixed-Inclined-Pad Thrust Bearings, ESDU (Engineering Science Data Unit) International Ltd, ISBN 0-85679-410-4, London, 1982, 42 p.

[3] Hamrock, B., Fundamentals of Fluid Film Lubrication, McGraw-Hill, Inc, 1994, 690 p.

[4] Lehtovaara, A., A Numerical Model for the Calculation of Transient Hydrodynamic Lubrication of Thrust Bearings, Finnish Journal of Tribology, 24(2005), 3-9.

[5] Lehtovaara, A., A Numerical Model for the Calculation of Transient Hydrodynamic Lubrication of Journal Bearings, Finnish Journal of Tribology, 25(2006), 14-22.

[6] Lehtovaara, A., A Numerical Model for Hydrodynamic Lubrication of Journal Bearings with Axial Lubricant Supply Groove and Axially Variable Geometry, Finnish Journal of Tribology, 26 (2007) 3-14.

[7] Stachowiak, G.W. and Batchelor, A.W., Engineering Tribology, Tribology Series, 24, Elsevier, The Netherlands, 1993, 872 p.

[8] Taguchi, G., System of Experimental Design, Vol 1 and 2, Unipub / Kraus Int. Publications, New York, 1987, 1189 p.